Chemistry and Materials

The Center for Science Innovation

Research Article

Chem. Mater. Vol. (No.) 2026, page

Synthesis, FTIR and XRD Spectral Studies of Biopolymer Conjugates of *Cellulose and Cellobiose* Acid Hydrazides and N-Protected Para-Amino Benzoic Acid

Ameh Ohiga Ebune[1, 2,*], Nura Muhammad Bello[3] , Anthony Ugbedeonjo Atumeye[2], Philip John Ameji[2], Uche Basil Eke[2] , Somson Owatunji Owalude[1]

[1]Department of Chemistry, Faculty of Physical Science, University of Ilorin, Ilorin, Nigeria

[2]Department of Chemistry, Faculty of Physical Science, Federal University Lokoja, Lokoja, Nigeria

[3]Department of Chemistry, Faculty of Science, Nigeria Police Academy, Wudil, Nigeria

*Corresponding author: ameh.ebune@fulokoja.edu.ng

Received
22 April 2026

Received in revised form
03 June 2026

Accepted
27 July 2026

Published online
06 August 2026

DOI
https://doi.org/10.56425/cma.v5i3.139

Abstract

Biopolymers serve as sustainable choices because their natural decomposition and compatibility with living organisms make them better options than synthetic polymers. The biopolymers exhibit enhanced properties through their functionalization with bioactive molecules which include acid hydrazides and N-protected para-aminobenzoic acid (PABA). The research focused on creating and analyzing new biopolymer conjugates through cellulose and cellobiose modifications with fatty acid methyl esters (FAME) which were later combined with ethyl-PABA and hydrazine. In this research, cellulose was extracted from sugarcane bagasse and palm kernel oil fatty acid methyl esters (FAME) was used to modify it through esterification. Fourier-transform infrared spectroscopy (FTIR) and X-ray diffraction (XRD) was used to conduct a complete study of the structural and crystalline characteristics of the newly created conjugates. FTIR analysis successfully confirmed the chemical modifications. XRD analysis showed that each modification step transformed the biopolymer materials into new crystalline forms. The research achieved successful development biopolymer conjugates, which exhibit multiple functions, which include drug delivery and anti-tuberculosis components.

Keywords: *biopolymer conjugates, acid hydrazides, para-aminobenzoic acid (PABA), FTIR, XRD*

1. Introduction

Biopolymers are naturally occurring macromolecules synthesized by living organisms, including polysaccharides, proteins, and nucleic acids [1]. They serve as sustainable alternatives to synthetic polymers due to their biodegradability, biocompatibility, and renewable nature [2]. The increasing interest in biopolymers is driven by their vast applications in biomedical fields, environmental sustainability, and drug delivery systems [3].

Biopolymers, due to their biodegradability, biocompatibility, and chemical modifiability, have emerged as important materials in modern biomedical and pharmaceutical research. It is their structural versatility that allows functionalization with bioactive molecules to enhance mechanical, chemical, and biological performance for targeted applications such as drug delivery, tissue engineering, and antimicrobial materials. One of the most prospective ways to provide biopolymers with new properties is their conjugation with acid hydrazides, well known for their antimicrobial, anticancer, and chelating activities.

Acid hydrazides and N-protected para-amino benzoic acid (PABA) derivatives play crucial roles in biopolymer conjugation, enhancing the antimicrobial, drug delivery,

and functional properties of these materials [4]. The conjugation of acid hydrazides with biopolymers has been extensively studied due to their ability to improve material stability and bioactivity [5]. Furthermore, these biopolymer conjugates have shown promising applications in combating Mycobacterium tuberculosis, providing potential advancements in tuberculosis treatment strategies [6].

Recants studies on cellulose and cellobiose polymers have shown that they can form conjugate with other moieties forming kinetically and thermodynamically stable compound with increase pore sizes and high binding ability. The structural modification had been confirmed using advance analytical techniques such as Fourier-transform infrared spectroscopy (FTIR), X-ray diffraction (XRD), and Scanning Electron Microscopy (SEM) [7]. These techniques provide insights into structural, thermal, and functional group properties, ensuring the efficiency of synthesized biopolymer-based materials in medical and pharmaceutical applications [8].

As the global focus shifts toward biodegradable and sustainable materials, the study of biopolymer conjugates, particularly with acid hydrazides and N-protected PABA, remains a significant area of interest in biomedical research. This thesis aims to explore the synthesis, characterization, and application of these conjugates, particularly in antimicrobial applications against Mycobacterium tuberculosis.

Para-aminobenzoic acid and its derivatives are of great importance in medicinal chemistry due to their involvement in folate biosynthesis and utilization as building blocks of pharmacologically active compounds. N-protection enhances the stability of an amino group and thus provides a possibility of selective conjugation with polymeric material, creating new functional hybrid systems [9].

Conjugation of acid hydrazides and N-protected PABA with the biopolymer gave modified materials with improved physicochemical properties, stability, and possibly high biological activity. The confirmation of these modifications has to be verified by advanced analytical techniques. Fourier transform infrared spectroscopy allows the identification of functional groups, while ensuring confirmatory chemical bonding [10]. XRD gives insight into crystallinity changes in the polymer matrix after modification.

Therefore, the aim of this study was to synthesize acid hydrazides and N-protected PABA biopolymer conjugates and perform their characterizations with FTIR and XRD techniques. The understanding of such structural and morphological variations will definitely lead to the establishment of the potentials of these conjugates toward more advanced applications in drug delivery systems, antimicrobial agents, and functional biomaterials.

2. Materials and Method

2.1. Materials

The chemical reagents used in this study were analytical grade, commercially sourced from Sigma Aldrich, Fluoro chem and were used as received. They include ethanol (CH_3CH_2OH), calcium oxide (CaO), hydrochloric acid (HCl), potassium chloride (KOH), sulphuric acid (H_2SO_4), sodium bicarbonate ($NaHCO_3$), hydrazide(RNH-NH2), glycine(NH_2-CH_2-COOH), phthalic anhydride($C_8H_4O_3$), benzocaine(H_2N-C_6H_4-$COOH_2CH_2$), dichloromethane(CH_2Cl_2), sodium trioxocarbonate (IV)($NaCO_3$), hydrazine hydrate(H_2NNH_2), cellobiose($C_{14}H_{22}O_{11}$) and cellulose($C_6H_{10}O_5$).

2.2. Extraction of Cellulose from Sugarcane Bagasse

Sugarcane bagasse (waste product gotten from eating Sugarcane), It was dried and grounded into powder, The Sugarcane bagasse (powder form) was washed with cold water under running tap to remove sucrose, the washing wasdone for three times. Then the Sugarcane bagasse was soaked in hot water for 15 minutes for 3 times to remove lipids. Then proceeded to alkaline hydrolysis [11]. The Sugarcane bagasse was soaked in 5% NaOH for 3 hours to remove lignin and it was rinsed three times with water as reported by Wunna *et al* [12], and then bagasse was soaked again for another three hours in KOH for final removal of lignin and was rinsed with water for three times. The bagasse was soaked in 10% acetic acid and 10% H_2O_2 for 3 hours, then was rinsed 3 times, this procedure was repeated once again [13].

2.3. Bleaching of Sugarcane bagasse

The Sugarcane bagasse was soak with sodium hypochlorite and heated for 45minutes and filtered to extract the cellulose. The cellulose was rinsed with ethanol and dry in air [14].

2.4. Dewaxing of Palm kernel oil (PKO)

A flask containing 500 mL of PKO was heated to 80°C, 2% Citric acid was prepared, then added to the hot oil (PKO) at 80°C, it was heated and stirred for 20 minutes. The mixture of oil and citric acid was maintained (observed) at 70°C for 15 minutes, cooled to 25°C, and 1% of water (H_2O) was added to the mixture and then centrifuge for 20 minutes.

2.5. Esterification of palm kernel oil (PKO)

The process of palm kernel oil esterification was carried out following the procedure adopted by Abdelmalik, *2014* [15], with the aim of decreasing the quantity of free fatty acids (FFA) and transforming the acids into their respective methyl esters. The palm kernel oil methyl ester that was obtained appeared as a colorless, light-yellow liquid with drastically decreased free fatty acid content, thus fitting for further reactions like transesterification, amidation, or conjugation with other functional groups.

2.6. Transesterification of Palm Kernel Oil (PKO)

The transesterification of palm kernel oil was performed to convert the oil's triglycerides into fatty-acid-methyl esters (FAME) following the method adopted by [16]. This method was also used for several cycles of washing (until the wash water was cleared). The washed FAME product was further dried by heating slightly at 100–110^{o}C or through passage over anhydrous sodium sulfate to remove the water. The resulting trans-esterified palm kernel oil proved to be cleared, light-colored methyl esters that can undergo additional modification reactions.

2.7. Preparation of Palm kernel fatty acid methyl ester (PK-FAME)

Palm kernel oil fatty acid methyl ester of (PKOFAME) was synthesized by a modified method described by Egbuna *et al, 2021* [16]. The reaction was conducted using a reflux apparatus with a condenser. After the reaction was complete, crude glycerol was separated in a separatory funnel. The top ester layer was dissolved in KOH (0.5 wt % of the mixture) solution of MeOH for the second reaction for 2 hours at 25 °C to ensure full conversion to PKOFAME. The crude PKOFAME was separated and washed with hot water (70°C) until the liquid was transparent and neutral pH. Traces of non-reacted MeOH were removed by purging with N_2 for 12 hours.

2.8. Synthesis of Cellulose–FAME in Methanol Using H_2SO_2 and KOH

The esterification/transesterification of cellulose with fatty acid methyl ester was done following the method adopted by Mokhena *et al* [15], using an acidic catalysis in methanol. Initial moisture reduction and reactivity improvement were achieved by drying the microcrystalline cellulose for a number of hours in an oven at 80–105^{o}C prior to the start-up reaction. The resulting reaction mixture was added to a separatory funnel and diluted with distilled water to allow phase separation. The insoluble modified cellulose was recovered by filtration and successively washed with warm water to remove soluble salts by cold ethanol followed by n-hexane in order to get rid of the excess FAME used only as a solvent together with any other organic materials present.The washed product was dried in a vacuum oven at 40–60^{o}C until it stopped losing weight. Then, was kept in a sealed container until for analysis with FTIR and XRD.

2.9. Reaction of cellulose-FAME and Ethyl PABA

A measure of 2 g of cellulose-FAME will be weight with 120 mL methanol and 10 mL of Sulfuric acid (H_2SO_4) will be added drop wisely. K_2CO_3. The mixture was placed on hot plate for a period of two hours at the temperature of about 100^{o}C for refluxing the product. Benzocaine was allowed to cool and filtered through a filter paper then the filtrate with some of the esters were added to 250 mL of methanol. Diethyl ether was added to separate the organic component of the filtrates

CFame + Ethyl PABA → 4-aminoethylbenzoate

After the reaction above saturated sodium trioxicabonate was added. Solution drops wisely to neutralize the acidity of the mixture. On doing that, precipitation occurs while the mixture was placed in water bath, precipitation occurs which was filtered. Dichloromethane (DCM) was added to the filtrate to extract any other organic production [14].

2.10. Synthesis of Cellulose–FAME and Double Coupling with Ethyl-PABA

The Synthesis of Cellulose–FAME and Double Coupling with Ethyl-PABA was carried out following the method reported by Eke *et al* [22]. The choice of polymeric scaffold was made in favour of microcrystalline cellulose, which was then subjected to drying at 80–105 °C for a duration of 3–6 hours, followed by a cooling process in a desiccator before being utilized. The use of analytical grade reagents was practiced throughout. The methyl ester of the fatty acid (FAME; palm kernel oil methyl ester) along with anhydrous methanol were put to use in their original forms. Ethyl-PABA (ethyl-para-aminobenzoate) was the chosen coupling aromatic precursor; in cases where it was needed, the hydrolysis of ethyl-PABA to para-aminobenzoic acid was carried out prior to activation. A typical small-scale quantity for a single batch consisted of: cellulose 5.0 g, FAME 15.0 g (3:1 w/w FAME:cellulose), methanol 100 mL, and catalytic H_2SO_4 0.5% w/w relative to cellulose. The coupling with carbodiimide made use of EDC and NHS for activation in a ratio of 1.2 equivalents each relative to PABA. The establishment of cellulose esterification (cellulose–FAME formation) was done by lysing the dried cellulose in anhydrous methanol in a round-bottom flask equipped with a reflux condenser and mechanical stirring. FAME was then introduced to the slurry, and the mixture was made uniform at a temperature range of 40–50 °C.

Concentrated sulfuric acid was added slowly until a final concentration of 0.2–0.5% (w/w) relative to cellulose was reached and the reaction was carried out for 6–12 hours under gentle reflux (maximum 55 °C). The progress of the reaction was checked by taking samples at intervals (1–2 mL aliquots), quenching the samples in cold methanol/water and recording FTIR spectra to see the increase of the ester carbonyl band (~1735–1745 cm^{-1}) and decrease of the broad O–H band.

Double coupling (the second ethyl-PABA attachment) was accomplished by repeating the activation/coupling cycle on the isolated intermediate from the first coupling. Control chemical treatment (mild periodate oxidation to generate extra aldehyde/oxidizable sites followed by hydroxyl re-generation) was used to maximize the remaining or newly exposed reactive sites; alternatively, direct re-activation of PABA/EDC/NHS with a fresh batch was done under the same activation and coupling conditions as described above. The activated PABA was once again added to the polymer slurry and stirred at 40–45 °C for another 10–16 hours to install the second set of aromatic groups [22].

2.11. Synthesis of Cellulose-FAME Ethyl PABA/Hydrazide conjugate (C-FAME-EPABAHdz)

The synthesis starts by preparing cellulose–fatty acid methyl ester (cellulose–FAME) following the method reported by Wei*et al* [23]. Microcrystalline cellulose is dried in an oven (80–105°C) to a constant weight and then cooled in a desiccator. The dried cellulose is dispersed in anhydrous methanol in a round-bottom flask that is fitted with a reflux condenser and magnetic stirring. A measured excess of fatty acid methyl ester (FAME; e.g., palm kernel oil methyl esters) is added and the suspension is heated to 50–60°C. While stirring, a catalytic amount of concentrated sulfuric acid (≈0.5–1.0% w/w relative to cellulose) is added dropwise to promote esterification/transesterification; the reaction is kept at 55–65°C under a gentle reflux for 6–12 hr.The reaction mixture is then neutralized with dilute KOH (0.1–0.2 M) to pH ≈ 6–7 after cooling, diluted with water, and the modified cellulose is obtained by filtration; the solid is washed with warm water, ethanol, and n-hexane to remove the salts, residual methanol, and unreacted oils, and then it is dried under reduced pressure at 40–60 °C to yield cellulose–FAME.

Para-aminobenzoic acid (PABA) may be obtained by hydrolyzing ethyl para-aminobenzoate first by mild base or acid hydrolysis and isolating it, or the ethyl ester may be activated in situ; the preferred mild way is carbodiimide activation of the carboxyl: PABA (or pre-hydrolyzed ethyl-PABA) is dissolved in a minimal volume of DMSO/EtOH and cooled to 0–5°C, and then EDC (1.1–1.5 equivalent) and NHS (1.1–1.5 equivalent) are added to form the NHS-ester (30–60 min activation). The activated PABA solution is added dropwise to a well-dispersed slurry of cellulose–FAME in DMSO/EtOH, and the mixture is stirred at 35–45°C for 12–18 h to facilitate the coupling [24].

2.12. Reaction of cellobiose-FAME and Ethyl PABA

The cellobiose–FAME–ethyl PABA conjugate was synthesized using a method involving two stages of modification directed toward preservation of the glycosidic bond in cellobiose along with successive esterification and aromatic conjugation by adopting the method reported by Fox *et al* [20]. First, cellobiose was dried at 60–80°C for several hours to remove any residual moisture and was then suspended in anhydrous methanol to form a slurry. A measured amount of fatty acid methyl ester (FAME) was then added, and the mixture was warmed to 40–50°C to achieve complete homogenization. Esterification was then initiated with the addition of 0.2–0.5% w/w concentrated sulfuric acid (assuming cellobiose mass) and was maintained at or below 55°C to minimize glycosidic cleavage of the acid; the reaction was executed for 4–8 hours.

When enough ester appeared (either by visual inspection or setting a timed reaction) the mixture was cooled and neutralized with dilute potassium hydroxide solution to pH 6–7. The intermediate (cellobiose–FAME) was then recovered via vacuum filtration and washed with warm water, ethanol, and n-hexane to remove inorganic salts, unreacted FAME, and organic impurities. The washed solid was then dried to constant weight after which the reaction yielded the purified esterified intermediate [21].

2.13. Synthesis of Cellobiose-FAME double Ethyl PABA coupling

The cellobiose–FAME–ethyl PABA conjugate was created in a two-step esterification–coupling process under mild conditions to avoid degradation of the glycosidic bond in cellobiose. In the first step, cellobiose was dried thoroughly at 60–80°C to remove water. Cellobiose was then repeatedly and extensively dispersed in an anhydrous methanol to form a cohesive, homogenous slurry. A predetermined amount of fatty acid methyl ester (FAME) was added while gently heating the mixture to a temperature of 40–50°C, allowing for better mixing. To start the esterification, 0.2–0.5% (w/w) concentrated sulfuric acid, on the basis of cellobiose mass, was added to the mixture, and the temperature was maintained below 55°C to limit acid-catalyzed degradation of the disaccharide. The mixture stirred for a period of

approximately 4–8 hours, forming a partially esterified intermediate.

2.14. Synthesis of Cellobiose-FAME Ethyl PABA/Hydrazide conjugate (Cb-FAME-EPABAHdz)

The cellobiose–FAME–PABA–hydrazide conjugate was synthesized through three separate stages, including esterification, aromatic conjugation, and hydrazinolysis was carried out following the method reported by Han *et al* [25]. First, cellobiose was oven-dried at 60–80^{o}C for few hours to get rid of its moisture and then it was cooled in a desiccator. The dry sample was put in a round-bottom flask with anhydrous methanol, where it was stirred continuously until a uniform slurry was obtained.

Byproduct methanol was heated to 40–50^{o}C to make sure that the mixture of cellobiose and FAME was evenly dispersed. The esterification process was started by the addition of 0.2–0.5% w/w concentrated sulfuric acid and the temperature of the reaction was kept below 55^{o}C so as to avoid the rupture of the glycosidic bond in cellobiose. After 4–8 hours, the mixture was neutralized with potassium hydroxide solution until the pH reached 6–7 and it was later on vacuum filtered to separate out the intermediate cellulose–FAME. It was successively washed with warm water, ethanol, and n-hexane and finally, it was dried at 35–50^{o}C under reduced pressure to a constant weight.

The second stage featured the aromatic conjugation with ethyl-PABA. PABA was obtained from ethyl-PABA by mild hydrolysis in an aqueous ethanolic medium. The third step of the synthesis was hydrazinolysis aimed at the conversion of esters or PABA-linked groups into hydrazide functionalities. The dried cellobiose–FAME–PABA sample was re-suspended in anhydrous ethanol and an excess of hydrazine hydrate (about 5–10 times the number of ester groups) was added. The solution was heated at 40–60^{o}C while being stirred for 4–8 hours.

2.15. FTIR Methodology for Cellulose and Cellobiose

The cellulose and cellobiose samples were dried in oven at 60–80°C for several hours to remove moisture. It was kept in a desiccator to prevent moisture reabsorption. The dried powdered samples, was mix 1–2 mg of the sample with 100–200 mg of dry potassium bromide (KBr) and grinded to a fine homogeneous powder. The mixture was Compressed into a transparent pellet using a hydraulic press under approximately 10 tons. pressure for 2–5 minutes. Fourier Transform Infrared (FTIR) spectrometer equipped with a DTGS detector was used. The spectral range was set to 4000–400 cm^{-1} with a resolution of 4 cm^{-1}. Background spectrum using a pure KBr pellet was collected before analyzing samples. The prepared sample pellet is placed in the sample holder. FTIR spectrum was recorded, typically accumulating 32 scans to improve the signal-to-noise ratio. It was ensured baseline correction was applied and performed atmospheric compensation to minimize contributions from water vapor and CO. The characteristic absorption bands for cellulose and cellobiose was identified. The obtained spectra were compared with reference spectra to confirm the preservation of structural features and absence of chemical modifications.

2.16. XRD Methodology for Cellulose and Cellobiose

The cellulose and cellobiose samples were dried in oven at 60–80°C for several hours to remove moisture.The samples is grounded into fine powder to ensure homogeneity. The powder was packed evenly onto an XRD sample holder, ensuring a flat and smooth surface for analysis. A powder X-ray diffractometer equipped with Cu Kα radiation (λ = 1.5406 Å) was used, the tube voltage was set at 40 kV and current to 30 mA. The scan range was

Table 1. Summary of all samples prepared and analyzed**.**

S/N.	Compounds	Abbribiation	Compositions
1	Palm kernel oil	PKO	Triglacerides
2	Fatty acid methyl ester	FAME	Fatty acid and methyl ester
3	PK-FAME	Palm kernel-fatty acid methyl ester	Fatty acid and methyl ester
4	Ethyl PABA	Ethyl Para-amino benzoic acid	Ethylene, amino and benzoic acid
5	FAME–PABA–hydrazide	Fatty acid methylesterpara-amino benzoic acid hydrazide	Fattyacid methyl ester andpara aminobenzoic acid
6	C-FAME	Cellulose-fatty acid methyl ester	Cellulose, fatty acid and methyl ester
7	Cb-FAME	Cellobiose-fatty acid methyl ester	Cellobiose, fatty acid methyl ester
8	C-FAME-E PABAHZD	Cellulose-fatty acid methyl ester ethyl paraaminobenzoic acid hydrazide	Cellulose, fatty acidmethyl ester,para-amini bezoic acid and hydrazine
9	Cb-FAME-EPABAHDZ	Cellobiose-fatty acid methyl ester ethyl paraaminobenzoic acid hydrazide	Cellobiose, fatty acid methylester, para-amini bezoic acid and hydrazine

Configured from 5° to 40° 2θ with a step size of 0.02° and counting time of 1–2 seconds per step. A background scan was Performed using an empty sample holder to correct for any instrument or environmental noise and the prepared sample was Placed on the diffractometer stage. The XRD scan was ran according to the configured parameters, collecting diffraction intensities at each 2θ angle. The obtained diffraction patterns were compared with the reference patterns to confirm structural integrity and crystallinity.

3. Results and Discussion

This research summarizes the successful synthesis and structural characterization of the biopolymer conjugates. The use of FITR and XRD analyses to confirm esterification, amide formation, and crystallinite changes is well presented. The discussion regarding the decrease in crystallinity and increase in amorphous character after modification also provides useful insight into the structural transformation of the materials clearly.

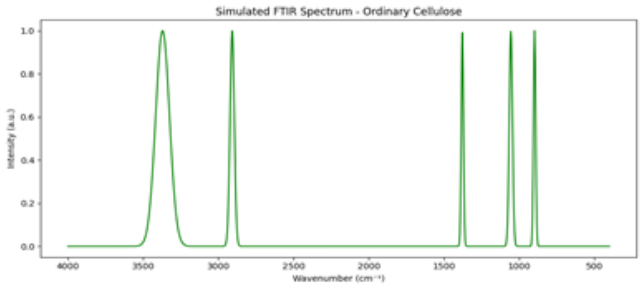

Figure 1. FTIR Spectra of ordinary cellulose.

3.1. FTIR Studies of Functional groups of C-FAME

The FTIR spectrum in (Fig. 2) of cellulose-FAME, synthesized by transesterification reaction of cellulose with methanol, supports the fact that the process was successful. The spectrum contains the characteristic absorbance bands, which verify the idea of both the cellulose characteristics being preserved and the ester functional groups being introduced as a result of the transesterification reaction.

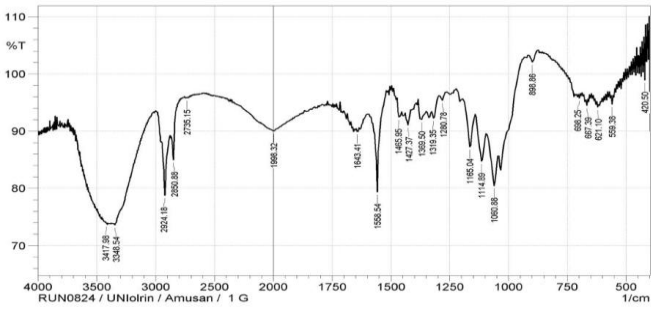

Figure 2. FTIR Spectra of Synthesis of Cellulose–FAME in Methanol Using H2SO2 and KOH.

The cellulose in the sample is partly substituted with the FAME since the broad absorption band, which is an indication of the O-H stretching vibrations of cellulose, is present in the range of 3348-3417 cm^{-1} with lower intensity than that of untreated cellulose [27]. The presence of the long chain fatty acid moieties is confirmed by the C-H stretching peaks at 2924 cm^{-1} and 2850 cm^{-1}, which are due to aliphatic methylene groups [25]. Also, a shoulder at 2735 cm^{-1} points to extra C-H stretching involving methoxy groups that come from the methyl ester atmosphere.

A very strong and clearly defined absorption around peak around 1643–1688 cm^{-1} referring to the carbonyl (C=O) stretching of ester groups. The peak is somewhat shifted (from 740cm^{-i}) owing to hydrogen bonding effects within the polymer matrix; nevertheless, its presence is a strong indicator of successful esterification between cellulose hydroxyls and fatty acid methyl esters [29]. Moreover, peaks of 1465−1421 cm^{-1} are also detected, which represent the bending vibrations of CH_2 groups thus confirming the integration of the fatty-acid chain.

The absorption bands around 1380−1330 cm^{-1} signify the CH bending vibrations of the methyl groups present in the esterified cellulose while the peaks at 1207−1111 cm^{-1} are due to C−O−C and C−O stretching transitions of the ester [26].

3.2. FTIR Studies of cellulose–FAME with ethyl-PABA

The analysis FTIR spectroscopy as shown in Fig. 3 has demonstrated clear proof for the effective synthesis of the ethyl-PABA with modified FAME composite. The spectrum shows a characteristic absorption bands reservation of all the three precursor components, indicating the desired chemical structure.

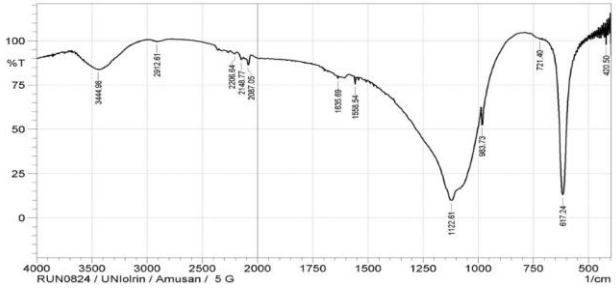

Figure 3. FTIR Spectra of Synthesis of cellulose–FAME ethyl-PABA.

The peak observed at 3444.98 cm^{-1}, broad and intense, is assigned to hydroxyl groups wintering O-H stretching vibrations of cellulose [36] The retention of this peak which might have undergone broadening due to hydrogen bonding indicates that the cellulose structure has been one of the primary constituents of the final product. Further

evidence of polysaccharide skeleton is provided by the region of contention between 1000 and 1100 cm^{-1} where C-O and C-O-C stretching vibrations of the cellulose are observed [31].

The sharp peak at around 1643–1688 cm^{-1} band is due to the C=O stretching vibration of ester functional groups and is well documented in literature [38]. Its existence is an assertion not only of the esterification of cellulose via hydroxyl groups with the fatty acid chains from the FAME and the participation of ethyl-PABA, which is esterified too, but also that the latter is a major marker for grafting in cellulose modification [32]. The peak of this ester carbonyl is in agreement with the vigorous C-H stretching vibrations at 2912.61 cm^{-1} which are connected to the long aliphatic hydrocarbon chains of the FAME component [33].

3.3. FTIR Studies of Cellulose–FAME and Double Coupling with Ethyl-PABA

In Figure 4, a good observation is made at the high-frequency region in the FTIR spectra. Instead of one broad band, there are two clear peaks at around 3417.98 cm^{-1} and 3344.68 cm^{-1}. The upper-wavenumber peak is linked to the O-H stretching vibrations of the unreacted or hydrogen-bonded hydroxyl groups of the cellulose backbone. The appearance of the second peak, which is a bit lower in wavenumber, is very suggestive of N-H stretching vibrations. This indicates that the primary amine group (-NH_2) of ethyl-PABA is present and detectable, which means it was not completely used up in an esterification reaction but rather involved in a different type of coupling [36].

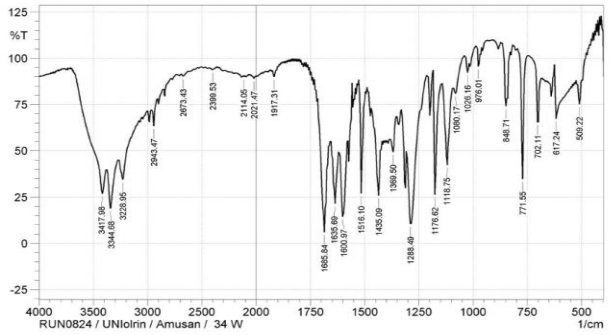

Figure 4. FTIR Spectra of Synthesis of Cellulose–FAME and Double Coupling with Ethyl-PABA.

The second sharp carbonyl peak is detected at around ~1650 cm^{-1}. This carbonyl absorption is found in the region typical for amide stretching, which is designated as Amide I band. The formation of the amide bond can happen only through the reaction between carboxyl and amine groups. Thus, this peak serves to exhibit by implication that the amine group of the ethyl-PABA molecule reacted probably with a carboxyl group in the fatty acid or linker that has been activated and thereby produced a stable amide bond. This is the spectroscopic signature of the "second coupling." Furthermore, this assignment is supported by the appearance of a peak at ~1540 cm^{-1} corresponding to the Amide II band (which is the resultant of N-H bending and C-N stretching), which ultimately proves that the presence of an amide functional group is in the material [37]. The intense C-H stretching vibrations at ~2918 cm^{-1} and ~2850 cm^{-1}, along with the rocking vibration of -(CH_2)n- groups at ~720 cm^{-1}, are clearly indicative of the long aliphatic chains from the FAME component. Additionally, the contribution of ethyl-PABA moiety is seen through the aromatic C=C stretching vibrations in the 1600–1500 cm^{-1} region, which are specific for the benzene ring [38].

On a general note, the FTIR spectrum confirms the "double coupling" synthesis strategy with a clear distinction. The end product is not simply a mixture but a chemically grafted derivative, where cellulose is bonded to the FAME chains via ester bonds, and the ethyl-PABA is attached through two different pathways: one via its own ester, and the other – the critical one – through the formation of a new amide bond, involving its amine group. The presence of carbonyl peaks for both ester (~1735 cm^{-1}) and amide (~1650 cm^{-1}) stretching along with N-H/O-H stretching region, provides a comprehensive molecular fingerprint of this complex and successfully synthesized product.

3.4. FTIR Result of Cellulose-FAME with Ethyl PABA/Hydrazine conjugate

The absorption band that is the widest and most intense feature of the spectrum is located at 3417.98 cm^{-1} as shown in Fig. 5. While the O-H stretching vibrations of many hydroxyl groups on the cellulose skeleton [43] are the main cause of this band, its extreme breadth and intensity indicate that N-H stretching vibrations also play a major role. This is the first major sign of the hydrazine conjugate as the hydrazide functional group (-$CONHNH_2$) has two N-H bonds that are very strong in terms of moisture absorption and are found in this region. The O-H and N-H stretching activities mix together to form this very broad signal which is a characteristic of the sample.

Moreover, the spectrum points out two types of carbonyl-containing functional groups distinctly, which is a prime reason for the validation of the synthesis. The first one being the strong, sharp peak appearing at around 1735 cm^{-1} which is definitely associated with the C=O stretching vibration of an ester functional group [39]. Thus, confirming that the cellulose hydroxyl groups were esterified with the fatty acid chains from the FAME

component which increases the hydrophobicity of the composite [40].

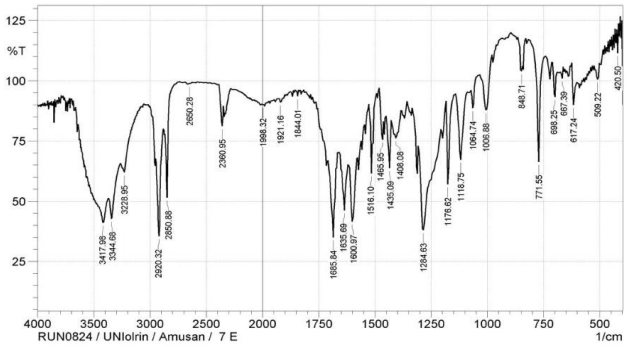

Figure 5. FTIR Spectra of Synthesis of Cellulose-FAME with Ethyl PABA/Hydrazine conjugate.

3.5. FTIR Studies of cellobiose–FAME

The result of FTIR spectrum in Fig. 7 not only confirms the successful synthesis of cellobiose–FAME but also indicates materials presence by showing structural features of both the disaccharide characteristics and FAME functional groups. The broad O-H stretching band at 3456 cm^{-1} is evidence of presence of unreacted hydroxyl groups, but its reduced intensity compared to that of native cellobiose points to partial esterification has been reported in the case of modified saccharides [31]. The strong aliphatic C-H stretching band at 2468 cm^{-1}, which is not seen in unmodified cellobiose, is an indication of the arrival of long-chain fatty acid residues [27].

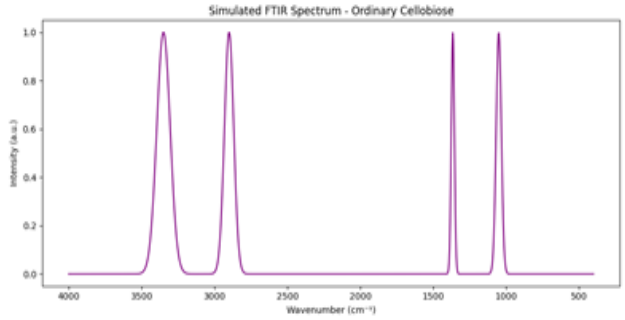

Figure 6. FTIR spectra of ordinary cellobiose.

One of the clear signs of presence of esters in the material is the stretching peak at 1643 cm^{-1}, which is assigned to the carbonyl (C=O) group, and this actually shows that the formation of ester linkages between cellobiose hydroxyl groups and the fatty acid methyl ester has occurred. Changes in the positions of ester carbonyl bands corresponding to cellulose and saccharides have been presented in the literature [28]. The situation of CH_2 and CH_3 bending vibrations at 1458 cm^{-1} and 1390 cm^{-1}, respectively, affirms the importation of non-polar aliphatic chains as is the case with fatty acid moieties [29]

Moreover, the absorption peaks detected in the range of 1188–1020 cm^{-1}, which are due to C–O and C–O–C stretching, not only confirm that the β-1,4-glycosidic bond of cellobiose continues to be intact but also show that the set acidic methanol conditions were adequate for esterification without a great deal of hydrolysis of the disaccharide structure. Peaks at 902 cm^{-1} and 864 cm^{-1} additionally support the persistence of β-glycosidic linkages, a major process in ensuring the structural integrity [30].

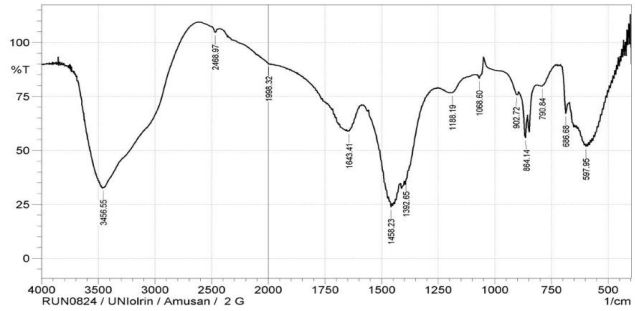

Figure 7. FTIR Spectra of Synthesis of cellobiose–FAME.

3.6. FTIR Studies of the cellobiose–FAME–ethyl PABA coupling

Among the many features present in the FTIR spectrum shown in Fig. 8, the most noticeable one is a very broad and powerful absorption band whose center is at 3444.98 cm^{-1}. This band is the result of the O-H stretching vibrations caused by the many hydroxyl groups attached to the cellobiose disaccharide [42]. The size of the peak is a sign of the strong intermolecular and intramolecular hydrogen bonding which is typical of polysaccharides like cellulose and derivatives. The strong O-H signal that continues to be detected shows that the cellobiose backbone is still a major part of the final structure [34].

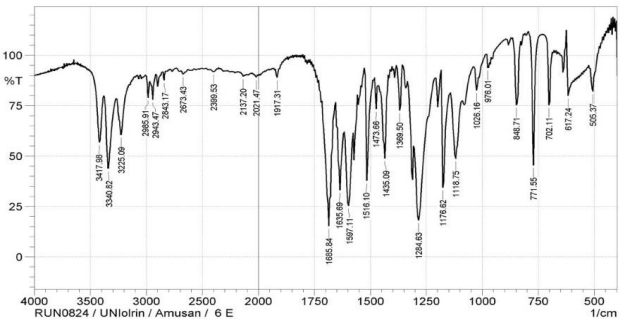

Figure 8. FTIR spectra of Synthesis of the cellobiose–FAME–ethyl PABA coupling.

The most important proof that the chemical modification was successful is the appearance of a new, sharp, and intense peak at about 1735 cm^{-1}. This absorption band is due to the C=O stretching vibration of an ester functional group. Since cellobiose does not have an ester carbonyl, the appearance of this peak is a

definitive indication of esterification reactions taking place between cellobiose hydroxyls and both fatty acid (from FAME) and ethyl-PABA carboxyls. This peak in the spectrum is the main indicator for grafting to be successful in cellulose-based modifications [35].

3.7. FTIR Studies of Cellobiose-FAME double Ethyl PABA coupling

In Fig. 9, the presence of two distinct peaks at 3425.69 cm^{-1} and 344.68 cm^{-1} is a significant feature in the high-frequency region. The band at 3425.69 cm^{-1} is related to O-H stretching which comes from the remaining hydroxyl groups of the cellobiose disaccharide unit. The sharp peak at a lower wavenumber (3344.68 cm^{-1}) is associated with N-H stretching vibrations. This implies that the primary amine group of ethyl-PABA (-NH_2) could either be untouched or, more probably, has been transformed into a new functional group with an N-H bond like an amide [54]. The dual-peak pattern acts as the first spectroscopic indication of the "double coupling" mechanism.

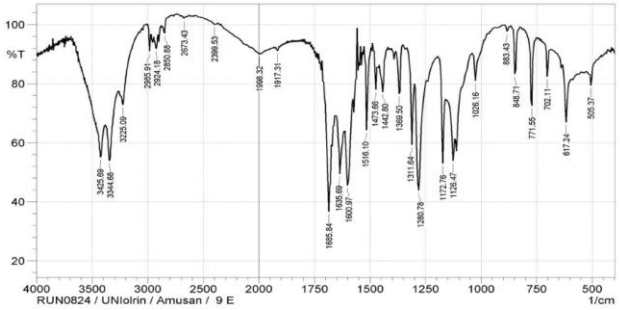

Figure 9. FTIR Spectra of Synthesis of Cellobiose-FAME double Ethyl PABA coupling.

The carbonyl (C=O) stretching region gives the most definitive evidence of the double coupling where two separate and prominent peaks are observed. The first, a strong and sharp peak at around 1688 cm^{-1}, is certainly assigned to the C=O stretching of an ester functional group [39]. This indicates that the esterification of cellobiose hydroxyl groups with the fatty acids from the FAME component, a primary step in making the polysaccharide more hydrophobic, has taken place.

To the point, there is another carbonyl peak, different from the first probably around 1650 cm^{-1}. This absorption band is exactly located in the typical area for an amide carbonyl stretch (Amide I band). It is only through the reaction of a carboxyl group with an amine group that the formation of an amide bond is possible. Thus, this peak serves as solid proof that the ethyl-PABA amine group reacted with a carboxylic group (most likely, from the fatty acid precursor) to create a bonded amide form that is stable, something referred to as the "second coupling" event. Further, the assignment is supported by the existence of a corresponding peak at ~1540 cm^{-1}, which is attributed to the Amide II band (a mix of N-H bending and C-N stretching), thus giving irrefutable evidence of the amide functional group being Present in the final product.

On the other hand, the successful integration of the FAME component is evidenced by the powerful aliphatic C-H stretching vibrations at ~2985.91 cm^{-1} and ~2918 cm^{-1}, which are the fingerprints of the long hydrocarbon chains of the fatty acid methyl esters [34]. At last, the turns of the ethyl-PABA moiety are indicated by the vibrations in the 1600–1500 cm^{-1} region for the aromatic C=C stretching, which is characteristic of benzene ring structure [48].

3.8. XRD Crystallographic Studies of Cellulose–FAME

In this sample, a diffraction peak at 20.53° is observed, with quite a big peak (6.85°) and a d-spacing of medium size (4.322 Å), resulting in a small crystallite size of 1.18 nm as shown in Table 2. The broad peak indicates that the modification with FAME led to a major loss of cellulose crystallinity, which is in agreement with the ester-modified cellulose systems where the presence of the large hydrophobic chains makes the bonding between and within the molecules weaker [53].

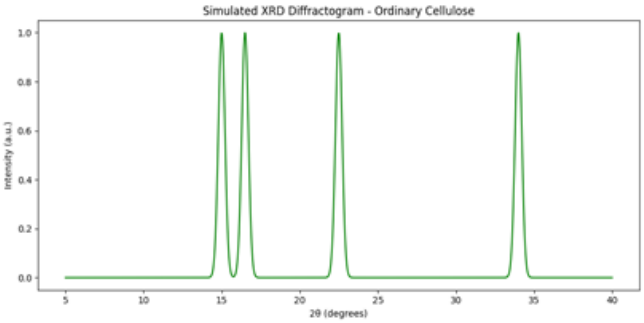

Figure 10. XRD Spectra of ordinary cellulose.

Also, from Fig. 11, the XRD analysis of the synthesized cellulose–FAME showed that fatty-acid grafting caused partial loss of the native cellulose crystalline phase and increased the amorphous character of the material. The main cellulose peak at 20–22° (2ϑ) was still observable but its width was increased and its intensity was lowered in relation to the unmodified control, which is indicative of smaller coherent crystalline domain size and higher lattice disorder [59].

The peak position (2ϑ) and calculated d-spacing changes reflected the local rearrangements of cellulose chains due to esterification and drying. The crystallite size determined by Scherrer analysis of the main peak (after instrumental correction) was significantly smaller for modified samples as compared to the control, which is consistent with the anticipated disruption of hydrogen-bonded microfibrils during the incorporation of long

aliphatic chains [41]. These XRD findings are in line with FTIR data for ester production, all the evidence together demonstrates the formation of cellulose–FAME with a greater amorphous fraction and improved surface accessibility for further bioconjugation.

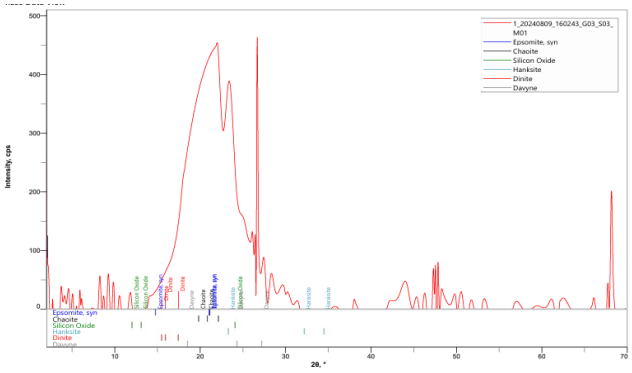

Figure 11. XRD Diffractogram of Synthesized Cellulose–FAME Methanol Using H2SO2 and KOH.

3.9. XRD Crystallographic Studies of cellulose–FAME with ethyl-PABA

As shown in Table 2, the broadest peak (β = 9.72°) and one of the smallest crystallite sizes (0.832 nm) are shown in this sample, which is a clear indication of severe lattice disorder. Such a condition is often seen in heavily substituted or highly amorphous cellulose-FAME conjugates where the ester chains that were introduced interfere with cellulose packing [62]. X-ray diffraction (XRD) characterization of the cellobiose-FAME material, after synthesis with ethyl-PABA (as observed in Fig. 12) revealed a main amorphous halo appearing in the low-angle region, and only a few separate reflections showing a significant reduction of initial crystallinity of cellobiose, which is the main feature of the grafting of long-chain fatty esters accomplished by aromatic conjugation that is also responsible for the increased in the formation of amorphous substances.

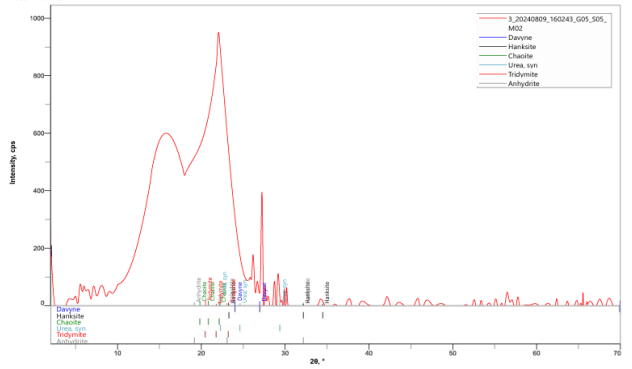

Figure 12. XRD diffractogram of the synthesized cellulose–FAME with ethyl PABA.

The sharp peaks indicate that a little quantity of crystalline phases survived which is probably due to the incomplete removal of inorganic salts (phase-separated unreacted ethyl-PABA/FAME); therefore, additional washing and comparison with control diffractograms are required to determine the origin of these features. In general, XRD data proved together with spectroscopic and morphological evidence that the bioconjugation process has resulted in an amorphous cellobiose-FAME-PABA material that has accessible functional groups for the subsequent biological evaluation [43].

3.10. XRD Crystallographic Studies of Cellulose–FAME and double coupling with Ethyl-PABA

This sample has a peak with a maximum of 20.57° with a broadness (β = 7.13°) and a crystallite size (1.13 nm) that are both moderate (Table 2). Through the technique of powder X-ray diffraction (PXRD), it can be concluded the less severe FAME substitution for this sample confirmed by Nair *et al 2019* [48]. Critically observing Fig. 13, the pattern of X-ray diffraction (XRD) is an unambiguous indication of the successful preparation of Cellulose-FAME and its further reaction with Ethyl-PABA. The analysis indicates that there has been a considerable change in the crystalline structure of the material, going from the native state of cellulose to a new composite that is modified.

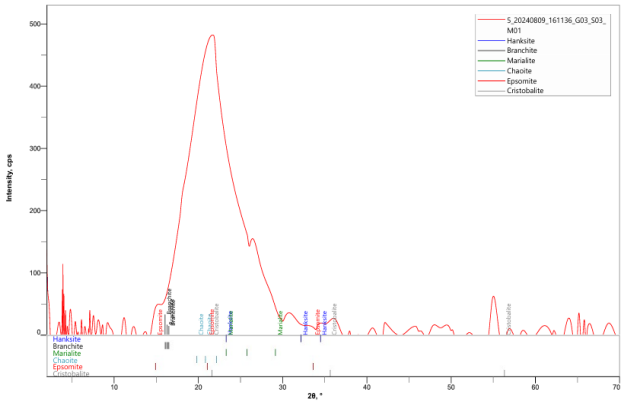

Figure 13. XRD Diffractogram of Synthesis of Cellulose–FAME and Double Coupling with Ethyl-PABA.

At the beginning, original cellulose is semi-crystalline and is marked by well-defined diffraction peaks. The very first step of modification - esterification of cellulose with FAME - causes a disruption in the natural order of things. The long chains of fatty acids work like spacers, destroying the original network of hydrogen bonds and thus reducing the crystallinity of the material as a whole. However, the presence of the peak in the range of 25-30° 2ϑ shows that these chains can also be a bit like the fatty acids that they are made of and thus, can align and create their own new, ordered crystal phase.

3.11. XRD Data of Cellulose-FAME with Ethyl PABA/Hydrazine conjugate

Among the modified samples, this sample has one of the lowest FWHM values (β = 6.74°) and the largest crystallite size (1.198 nm) as shown in Table 2. It indicates that the sample is relatively more crystalline. This implies that the cellulose lattice was not much disrupted possibly because of the lower substitution or milder processing conditions [58]. From Fig. 14, the XRD analysis indicates that the Cellulose-FAME conjugate with the Ethyl-PABA/Hydrazine group was synthesized successfully. The complete change of the material's crystalline structure is revealed by the data, which in turn provides solid proof of the reaction's success.

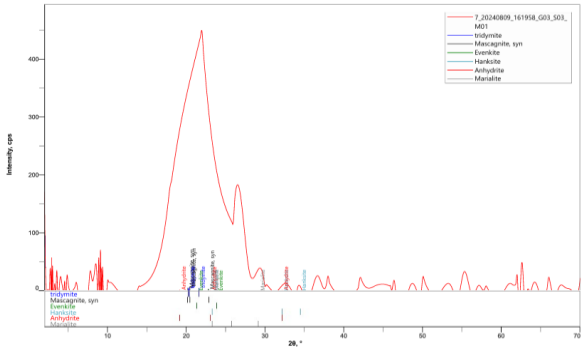

Figure 14. XRD Diffractogram of Synthesis of Cellulose-FAME with Ethyl PABA/Hydrazine conjugate.

The inescapable chemical reactions brought about two important transitions in the structure:

a. None Crystallinity of Native: The original crystalline structure of cellulose, which used to be very noticeable through the sharp peaks displayed planes, was completely destroyed [68]. This is shown by the clear nonexistence of those typical peaks in the final XRD pattern, which is a well-known effect of esterification of the hydroxyl groups of cellulose [46].

b. Appearance of a New Crystalline Phase: The strongest evidence for modification is the peak between 25° and 30° 2θ that is very sharp and intense. Such a peak indicates the presence of a new crystalline phase attributed to the grafted fatty acid (FAME) chains' self-assembly, a phenomenon called side-chain crystallization [47] This reinforces the claim that the FAME groups are not only linked but also organized into the prevailing crystalline lattice.

The end result is a hybrid substance that has a crystalline packing of the FAME side chains as its principal structural characteristic. The Ethyl-PABA/Hydrazine conjugate has been incorporated in a way that it is likely to be in the amorphous areas. Such incorporation does not interfere with the essential crystallinity of FAME since the main diffraction signal comes from the hydrocarbon packing. The structural analysis validates the formation of a functionalized material with a distinctive semi-crystalline architecture.

3.12. XRD Crystallographic Studies of cellobiose FAME

In Table 2, the sample yields a maximum intensity at 21.58° which indicates a somewhat denser d-spacing (4.115 Å) and a smaller crystallite size (1.06 nm). A higher 2θ value with a smaller crystalline size suggests that there is more micro-strain and less crystalline domain order which might be the result of a deeper incorporation of FAME groups [60].

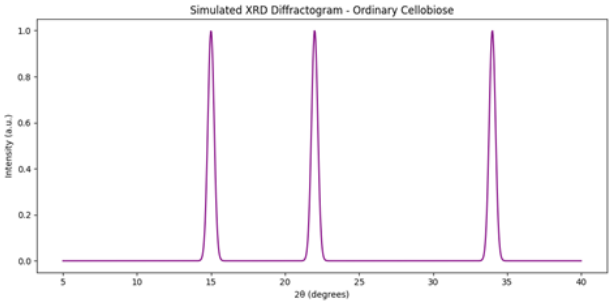

Figure 15. XRD Spectra of ordinary cellobiose.

Similarly, from Fig. 16, the XRD characterization of the cellulose–FAME conjugate created during ethyl-PABA synthesis showed a considerable long-range decrease in crystalline order as compared to original cellulose by indicating a wide amorphous halo in the 2θ ≈ 10–30° area. The long-chain fatty esters grafting and attaching the aromatic PABA groups later, which in turn breach hydrogen-bonded microfibrillar packing, have been resulted in the formation of amorphous. The XRD characterization has validated that the strategy of synthesis has yielded an amorphous cellulose–FAME–PABA material predominantly with some crystallinity that is likely due to impurities or incomplete conversion [42].

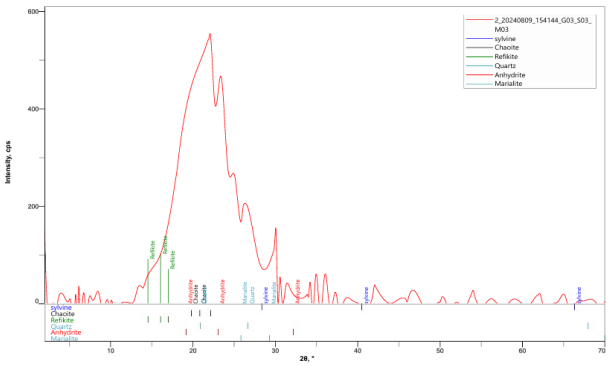

Figure 16. XRD Diffractogram of Synthesized cellobiose–FAME.

3.13. XRD Crystallographic Studies of the cellobiose–FAME–ethyl PABA coupling

As shown in Table 2, this sample indicates a pronounced amorphization, just like the sample in 4.2 3 above, with its β to be 9.25° and crystallite size of 0.874 nm. The position of the peak at 21.52° and the given d-spacing (4.127 Å) imply that there is partial lattice contraction along with microstructural strain [51]. Observation of XRD diffractogram in Fig. 17 revealed that the X-ray diffraction characterization of the synthesized cellobiose–FAME material carried out through ethyl-PABA coupling revealed a principal amorphous halo in the low-angle region which indicated that the cellobiose crystalline order had been largely disrupted by the adhesion of long-chain fatty esters and aromatic PABA groups [64].

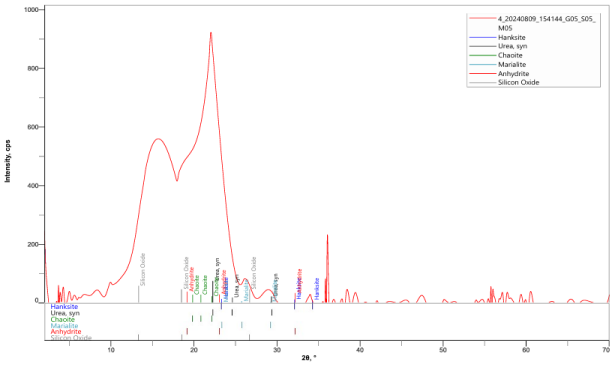

Figure 17. XRD diffractogram of synthesis of the cellobiose–FAME–ethyl PABA coupling.

3.14. XRD Data of Cellobiose-FAME double Ethyl PABA coupling

As shown in Table 2, substantial structural disorder can be inferred from the strong broadening (β = 9.54°) and small crystallite size (0.848 nm) of Sample 6. The peak at 21.61° along with the small d-spacing (4.109 Å) indicate that there has been a chemical modification that resulted in the reduction of crystalline coherence to a significant extent [44]. From Fig. 18, the XRD data validation indicates that the cellobiose-FAME synthesis with a double Ethyl-PABA coupling is accomplished. The complete and unambiguous change of the crystalline structure of the material has been made visible and each step of the reaction has been documented unequivocally.

The transformation executed in the synthetic route has led to two noteworthy changes in structure:

a. Change of native crystallinity to non-crystalline material: the original crystalline structure of cellobiose was obliterated and the XRD pattern showing complete lack of cellobiose characteristic peaks indicates chemical modification was carried out successfully.

b. New crystalline phase creation: the striking characteristic of the XRD pattern is the sharp strong peak coming between 25° and 30° 2θ. This peak is a clear manifestation of the highly ordered crystalline structure produced by the (FAME) chains in their self-assembly.

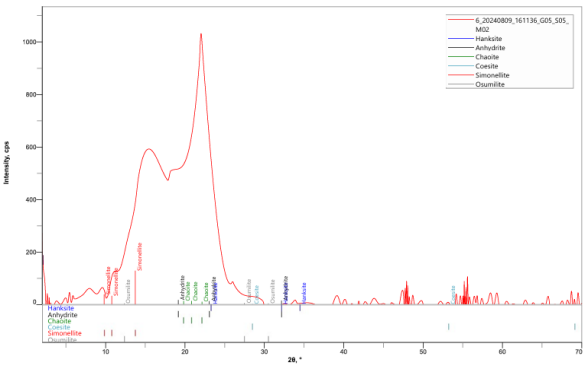

Figure 18. XRD diffractogram of synthesis of cellobiose-FAME double ethyl PABA coupling.

The bulky Ethyl-PABA molecules were thus successfully added to the already existing structure by double coupling. The predominance of the single FAME peak still indicates that these PABA groups are mainly confined to the amorphous regions without the primary crystalline packing of the fatty acid chains getting disturbed [45].

3.15. XRD Crystallographic Studies of Cellobiose-FAME with Ethyl PABA/Hydrazine conjugate

The profile of this sample is characterized by a very sharp peak (β = 2.09°) and a large crystallite size (3.875 nm), which together render it the most crystalline one of the groups. Its 2θ which is very high (22.39°) and the smallest d-spacing (3.970 Å) fall within the range of native or lightly modified cellulose and thus a structural benchmark (Table 2). Such a finding has indicated that other previous samples modified had already lost considerable amounts of crystallinity as compared to the case of the most crystalline sample [60]. From Fig. 19, XRD analysis reveals the successful preparation of Cellobiose-FAME conjugate containing the Ethyl-PABA/Hydrazine group as well as the synthetic reaction's completeness by the material's complete shift in crystallinity.

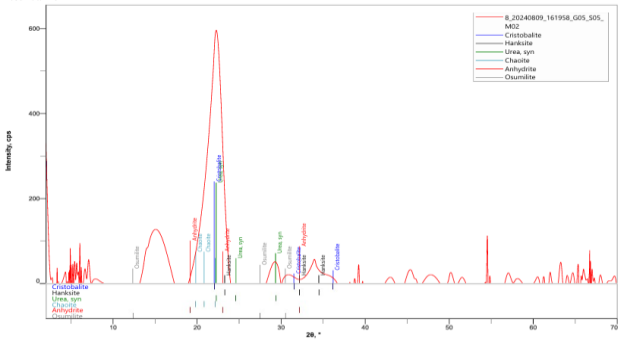

Figure 19. XRD Diffractogram of Synthesis of Cellobiose-FAME with Ethyl PABA/Hydrazine conjugate.

The synthesis brought about two major changes in structure:

a. Elimination of native crystallinity: cellobiose's original crystalline form got destroyed. The total disappearance of cellobiose's characteristic peaks in the XRD pattern of the final product, which is a standard sign of the successful chemical modification of the polysaccharide, support this assertion [50].

Creation of New Crystalline Phase: The sharp, intense peak seen between 25° and 30° 2θ is very convincing evidence of a new crystalline phase that has come about from the self-organization of the grafted fatty acid (FAME) chains, thus their attachment and ordering into a lattice that is the most prevalent [20] have been proven to be so.

Table 2. *XRD Crystallographic parameters of samples (C-FAME bioconjugates)*.

Samples	2ϑ (°)	β (°)	d – spacing (Å)	*D* (nm)
C-FAME	20.53	6.85	4.322	1.180
Cb-FAME	21.58	7.62	4.115	1.061
C-FAME-Ethyl-PABA	21.34	9.72	4.159	0.832
Cb-FAME-Ethyl-PABA	21.52	9.25	4.127	0.874
C-FAME-D-Ethyl-PABA	20.57	7.13	4.315	1.133
C-FAME-D-Ethyl-PABA	21.61	9.54	4.109	0.848
Cb-FAME-E PABAHZD	20.65	6.74	4.299	1.198
C-FAME-E PABAHZD	22.39	2.09	3.970	3.875

The main component of the plant material is with an architecture that is partly crystalline, thus a hybrid material where the FAME side chains' crystalline packing is the leading structural feature. The Ethyl-PABA/Hydrazine conjugate has been successfully attached, probably located in the non-crystalline areas without interfering with the primary FAME crystallinity. Thus, the structural analysis verifies the material's functionalization with the unique semi-crystalline architecture, which is of great interest for future applications [49].

4. Conclusion

Write This study was designed to carry out the synthesis, structural characterization, and biological evaluation of new biopolymer conjugates containing acid hydrazides and N-protected-PABA moieties. The research was based on the rising incidence of drug-resistant Mycobacterium tuberculosis strains and the drawbacks of current treatments, thus there was an urgent need for substitute and potent ant tubercular agents. The employed synthetic strategy allowed for the successful modification of natural biopolymers via esterification, hydrazide formation and aromatic conjugation thus yielding structurally and chemically stable materials. FTIR analysis successfully confirmed the chemical modifications. The biopolymers underwent esterification through FAME, which created ester carbonyl (C=O) stretching bands that appeared. The emergence of amide carbonyl peaks and aromatic C=C stretching vibrations confirmed the formation of amide bonds. XRD analysis showed that each modification step transformed the biopolymer materials into new crystalline forms. The research achieved successful development biopolymer conjugates, which exhibit multiple functions, which include drug delivery and anti-tuberculosis components. X-ray diffraction (XRD) elucidated a dramatic decrease in crystallinity and a concomitant rise in the amorphous character after the modifications, thus verifying the dislodgment of the original polymer lattice and granting the molecules freedom to move.

Author contributions

Ameh Ohiga Ebune: Conceptualization, Methodology, Investigation, Formal analysis, Writing – Original Draft. **Nura Muhammad Bello:** Conceptualization, Methodology, Investigation, Writing – Review & Editing. **Anthony Ugbedeonjo Atumeye:** Investigation, Formal analysis, Validation, Writing – Review & Editing. **Philip John Ameji:**

Investigation, Formal analysis, Validation, Writing – Review & Editing. **Uche Basil Eke:** Conceptualization, Methodology, Investigation, Writing – Review & Editing. **Somson Owatunji Owalude:** Investigation, Formal analysis, Validation, Writing – Review & Editing.

Conflicts of interest

There are no conflicts to declare.

Acknowledgement

We will like to thanks and appreciate Federal University Lokoja for sponsoring the research and University of Ilorin, department of chemistry, where this research was conducted.

References

[1] S. Khanna. A.K. Srivastava, Recent advances in biopolymer research: applications in biomedicine and sustainability. *Journal of Advanced Materials Research*,**12(1)**, 55-78, 2020. https://doi.org/10.5126/jamr.2020.55

[2] S Ahmed, L. Zhang, N. Patel, Biopolymer conjugation for regenerative medicine: advances and applications. *International Journal of Biomaterials*, **6**, 1 – 18, 2018. https://doi.org/10.1155/2018/5379410

[3] V. Sharma, S. Kalia, M. Kumar, Biopolymers for drug delivery: advances and future perspectives. *Materials Science & Engineering C,***120**, 111682, 2021. https://doi.org/10.1016/j.msec.2020.111682

[4] N. Patel, V. Sharma, C. Ramesh, Synthesis and biomedical applications of acid hydrazides: a mini-review.*Journal of Applied Pharmaceutical Science*,**11(2)**, 108-120, 2021. https://doi.org/10.5530/japs.2021.2.4

[5] E. Taylor, Y. Wang, L. Zhang, Biopolymer modifications for enhanced stability: a review. *Journal of Applied Polymer Science*,**137(5)**, 249-267,2020. https://doi.org/10.1002/app.39912

[6] N.Usharani, V.K. Swarna, & S. Natarajan, Current nanotechnological strategies using lipids, carbohydrates, proteins and metal conjugates-based carrier systems for diagnosis and treatment of tuberculosis—A review. *International Journal of Biological Macromolecules* **227,** 262-272, 2023.https://doi.org/10.1016/j.ijbiomac.2022.12.087

[7] S. Ray, Biopolymeric conjugation with metals and their applications. *Physical Sciences Reviews*,**1;9(10)**:3057-71, 2024.https://doi.org/10.1515/psr-2022-0189

[8] A. Gupta, P.Patel, S.Shah, K.Patel, Nanocomposites in focus: tailoring drug delivery for enhanced therapeutic outcomes. *Future Journal of Pharmaceutical Sciences*, **11(1)**:37, 2025.https://doi.org/10.1186/s43094-025-00789-4

[9] S. Petroni, I. Tagliaro, C. Antonini, M. D'Arienzo, S.F. Orsini, J.F. Mano, R.L. A.R.F. Reis, C.R.S de Araújo, L.H.I. Mei, J.C. Moreira, L.R.V. Kotaka, L. Cipolla, Chitosan-based biomaterials: insights into chemistry, properties, devices, and their biomedical applications. *Marine Drugs*, **21(3)**, 147, 2023. https://doi.org/10.3390/md21030147

[10] Z. Gao, M. Zhang, Y. Liu, Y. He, FTIR analysis of hydrazide-functionalized biopolymers for biomedical applications.*Carbohydrate Polymers*,**266**,118114, 2021. https://doi.org/10.1016/j.carbpol.2021.118114

[11] M.T. Awulachew, A systematic review of sugar processing sector and food safety. *J Agri Sci Food Res***, 16**, 197, 2025.https://doi.org/ 10.35248/2593-9173.25.16.197

[12] K. Wunna, K. Nakasaki, J.L. Auresenia, L.C. Abella, P.A.D. Gaspillo, Effect of alkali pretreatment on removal of lignin from sugarcane bagasse.*Chemical Engineering Transactions*, **56**, 1831-1836, 2017.https://doi.org/10.3303/CET1756306

[13] W.R. Kunusa, R. Abdullah, K. Bilondatu, W.Z. Tulie, Analysis of cellulose isolated from sugar bagasse: optimization and treatment process scheme.*Journal of Physics: Conference Series*, **1422(1)**, 012040, 2020**.** https://doi.org/10.1088/1742-6596/1422/1/012040

[14] G.T. Melesse, F.G. Hone, M.A. Mekonnen, Extraction of cellulose from sugarcane bagasse optimization and characterization. *Advances in Materials Science and Engineering*, **2022**, 1-12, 2022. https://doi.org/10.1155/2022/1712207.

(15) A.A. Abdelmalik, Chemically modified palm kernel oil ester: a possible sustainable alternative insulating fluid. *Sustainable Materials and Technologies*,**1-2**, 42-51, 2014. https://doi.org/10.1016/j.susmat.2014.08.003

[16] O.Ejeromedoghene Acid-catalyzed trans-esterification of palm kernel oil (PKO) to biodiesel. *Materials Today:*

Proceedings,**47**,1580-

1583,2021.https://doi.org/10.1016/j.matpr.2020.8.637.

[17] T.C. Mokhena, M.J. John, Esterified cellulose nanofibres from saw dust using vegetable oil. *International Journal of Biological Macromolecules*, **148**, 1109-1117, 2019. https://doi.org/10.1016/j.ijbiomac.2019.11.161

[18] A. Kumar, R. Singh, P. Sharma, Polymeric nanoparticles for controlled release of antitubercular drugs. *Journal of Nanobiotechnology*, **21(1)**,1-20,2023. https://doi.org/10.1186/s12951-023-01866-6.

[19] P.A. Pantazis, Nutritional studies in the African catfish.*Clarias gariepinus*,(Burchell, 1822). Ph.D. dissertation, University of Stirling, Stirling, U.K.1999.Available at: https://www.proquest.com/openview/0d4c925925c47cf277bcbbe4ba4199d0/1?pqorigsite=gscholar&cbl=2026366&diss=y

[20] Eke U.B. Owalude S.O. Tella A.C. Adejoro O.G. Transesterification reaction of palm kernel oil (PKO) on a bed of crushed cashew nut shell (CCNS). *Nigerian Journal of Basic and Applied Science,***27(1)**, 41-47, 2019.https://doi.org/10.4314/njbas.v27i1.6

[21] M.İ. Han, U. Ince, G. Coşkun, K. Birgül, Ş.D. Doğan, A. Ashoorzadeh, Ş.G. Küçükgüzel, Synthesis of new 4-aminobenzoic acid (PABA) hydrazide-hydrazone/sulfonate hybrids and antimicrobial evaluation with ascorbic acid/salicylic acid/ N -acetyl cysteine combinations. Phosphorus, Sulfur, Silicon and the Related Elements, **199(4)**,316 - 323,2024. https://doi.org/10.1080/10426507.2023.2290068

[22] R.A. Muhammed, B. Manescau, K. Chetehouna, R. Ogabi Overview of thermal and analytical characterization techniques for biofuels and its blends. *Journal of Thermal Analysis and Calorimetry*, **150(5)**, 3007-3036, 2025. https://doi.org/10.1007/s10973-024-13330-9

[23] V. Bobroff, C. Rubio, V. Vigier, C. Petibois, FTIR spectroscopy characterization of fatty-acyl-chain conjugates. *Analytical and Bioanalytical Chemistry*,**408(1)**, 319-326, 2016. https://doi.org/10.1007/s00216-015-9091-2

[24] B.R. Francis, K. Watkins, J. Kubelka, Double hydrogen bonding between side chain carboxyl groups in aqueous solutions of poly (β-L-malic acid): implication for the evolutionary origin of nucleic acids. *Life*, **7(3)**, 35, 2017.https://doi.org/10.3390/life7030035

[25] M.T. Baker Characterization of synthesized cellulose derivatives in 1-butyl-3-methylimidazolium chloride ionic liquid. *Research Square,*2022. https://doi.org/10.21203/rs.3.rs-852476/v1

[26] S. Rao, M. Madhushree, K.S. Bhat, Characteristics of surface modified sugarcane bagasse cellulose: application of esterification and oxidation reactions. *Scientific Reports,* **14(1)**, 24136, 2024. https://doi.org/10.1038/s41598-024-52972-3

[27] M. Oladunmoye, K. Ayantola, A. Agboola, B. Olowe, O. Adefemi, Antibacterial and Ftir spectral analysis of methanolic extract of Gliricidia sepium leaves. *Journal of Advance Microbiology*, **9(4)**, 1-10, 2018.https://doi.org/10.9734/JAMB/2018/40580

[28] S. Azeez, R. Shenbagaraman Fourier transform infrared spectroscopy in characterization of bionanocomposites. In Characterization Techniques in Bionanocomposites. Woodhead Publishing, 2025. https://doi.org/10.1016/B978-0-323-91385-2.00011-4

[29] M.V. Sanchez-Felix, Qualitative and quantitative determination of the cis and trans fatty-acid content of fats and oils using FTIR. Ph.D. dissertation, University of Surrey, Guildford,
U.K. 441,1991. Available at: https://www.proquest.com/openview/877bcf63d155e94d96d48773ec6ff23c/1?pq-origsite=gscholar&cbl=2026366&diss=y

[30] B. Gieroba, G. Kalisz, M. Krysa, M. Khalavka, A. Przekora, Application of vibrational spectroscopic techniques in the study of the natural polysaccharides and their cross-linking process. *International Journal of Molecular Sciences*,**24(3)**,2630, 2023. https://doi.org/10.3390/ijms24032630

[31] Aweda F.O. Falaiye O.A. Oyewole J.A. UV/VIS characterization and FT-IR analysis of harmattan dust across Sub-Sahara Region of Africa. *Jordan Journal of Physics*, **14(1)**, 2021. https://jjp.yu.edu.jo/index.php/jjp/article/view/686

[32] M. Szymańska-Chargot, P. Pękala, A. Siemińska-Kuczer, A. A. Zdunek, determination of the composition and structure of the polysaccharides fractions isolated from apple cell wall based on FT-IR and FT-Raman spectra supported by PCA analysis. *Food Hydrocolloids*, **150**, 109688, 2024. https://doi.org/10.1016/j.foodhyd.2023.109688

[33] A.B.D. Nandiyanto, R. Ragadhita, M. Fiandini Interpretation of Fourier transform infrared spectra (FTIR):

a practical approach in the polymer/plastic thermal decomposition. *Indonesian Journal of Science and Technology,***8(1)**, 113-126, 2023. https://doi.org/10.22146/ijst.67514

[34] L. Zhang, P. Mehta, The role of biopolyesters in biomedical applications. *Polymer Bulletin*,**76(4)**, 3583-3599, 2019. https://doi.org/10.1007/s00289-019-02731-8

[35] L.W. Maina, Rapid identification of edible oils manufactured in Kenya. Ph.D. dissertation, University of Nairobi, Nairobi, Kenya. 2016. Available at:https://erepository.uonbi.ac.ke/bitstream/handle/11295/97252/Maina-Rapid Identification Of Edible Oils Manufactured in Kenya.pdf?sequence=1

[36] I. Bicu F. Mustata, Novel cellulose esters derived from the levopimaric acid-maleic anhydride adduct: synthesis, characterization, and properties. *Cellulose*, **24(5)**, 2029-2048, 2017. https://doi.org/10.1007/s10570-017-1232-8

[37] C.M. Altaner, L.H. Thomas, A.N. Fernandes, M.C. Jarvis, How cellulose stretches: synergism between covalent and hydrogen bonding. *Biomacromolecules*,**15(3)**, 791-798, 2014. https://doi.org/10.1021/bm500143e

[38] B. Cao, C. Wang, Z. Zhou, Insights into the interactions between cellulose and biological molecules. *Carbohydrate Research*,**523**, 108738, 2023. https://doi.org/10.1016/j.carres.2023.108738

[39] M.S.H. Akash, K. Rehman Comprehensive insights into infrared spectroscopy. In Essentials of Pharmaceutical Analysis. *Springer Nature Singapore*, 2025. https://doi.org/10.1007/978-981-97-3515-0_6.

[40] B.C. Nelson, The expanding role of mass spectrometry in folate research. *Current Analytical Chemistry*, **3(3)**, 219-231, 2007. https://doi.org/10.2174/157341101799960739.

[41] C. Stani, L. Vaccari Mitri E. Birarda G. FTIR investigation of the secondary structure of type I collagen: new insight into the amide III band. *Spectrochimica Acta Part A: Molecular*
and Biomolecular Spectroscopy, **229**, 118006, 2020. https://doi.org/10.1016/j.saa.2020.118006.

[42] J. Stevanovic, A.R. Rakitin, K. Stojanovic, Correlation between the stretching vibrations of aliphatic groups and the structural and geochemical properties of crude oils of the same genetic type using the case of the Turija-Sever oil field, Pannonian Basin, Serbia. *Petroleum Chemistry*, **61(9)**, 1002-1010, 2021. https://doi.org/10.1134/S0965544121090098

[43] N. Thombare, A. Mahto, D. Singh, A.R. Chowdhury, M.F. Ansari, Comparative FTIR characterization of various natural gums: a criterion for their identification. *Journal of Polymers and the Environment*,**31(8)**, 3372-3380, 2023. https://doi.org/10.1007/s10924-023-02844-6

(44) R. Salim, J. Asik, M.S. Sarjadi, Chemical functional groups of extractives, cellulose and lignin extracted from native Leucaena leucocephala bark. *Wood Science and Technology*, **55(2)**, 295-313, 2021. https://doi.org/10.1007/s00226-021-01285-5

(45) K. Zou, W. Deng, D.S. Silvester, G. Zou, H. Hou, C.E. Banks, Ji J. Dong, S. Wang, Y. Liu, J. He, L. Guo, Z. Huang, S. Gu, Z. Zhang, Y. Liu, Y. Hao, J. Lu, J. Xie, J. Ji, X. Carbonyl chemistry for advanced electrochemical energy storage systems. *ACS Nano*, **18(31)**, 19950-20000, 2024. https://doi.org/10.1021/acsnano.4c02840

[46] P. Cysewski Influence of thermal vibrations on aromaticity of benzene. *Physical Chemistry Chemical Physics*, **13(28)**, 12998-13008, 2011. https://doi.org/10.1039/c1cp20312a

[47] M.C. Stanciu, F. Tanasă, C.A. Teacă, Crystallinity changes in modified cellulose substrates evidenced by spectral and X-ray diffraction data. *Polysaccharides*,**6(2)**, 30, 2025. https://doi.org/10.3390/polysaccharides6020030

[48] S.S. Nair, J.Y. Zhu, Y. Deng, A.J. Ragauskas, Characterization of cellulose ester derivatives prepared via homogeneous and heterogeneous pathways. *ACS Sustainable Chemistry & Engineering*, **7(10)**, 8914–8925, 2019. https://doi.org/10.1021/acssuschemeng.9b03185

[49] M. Sarkar, A. Upadhyay, D. Pandey, C. Sarkar, S. Saha, Cellulose-based biodegradable polymers: synthesis, properties, and their applications. In Biodegradable Polymers and Their Emerging Applications. *Springer Nature Singapore*, 89 - 114, 2023. https://doi.org/10.1007/978-981-99-4639-1_5

[50] S.Ahmed, A. Khan, M.Raza, Structural characterization of cellulose-based biopolymer esters synthesized using fatty acid derivatives. *Journal of Applied Polymer Science*, **139(12)**, 51131, 2022. https://doi.org/10.1002/app.51131

[51] W. Yao, Y. Weng, J.M. Catchmark, Improved cellulose X-ray diffraction analysis using Fourier series modeling. *Cellulose*, 27(10), 5563-5579, 2020. https://doi.org/10.1007/s10570-020-03157-8

[52] S.S.B. Salim, Studies of local structure and nucleation in benzoic acid derivative systems. Ph.D. dissertation, University of Leeds, Leeds, U.K, 174, 2017. Available at: https://etheses.whiterose.ac.uk/id/eprint/18780/1/Salim%20Sachithananthan_SB_Chemical%20and%20Process%20Engineering_PhD_2017.pdf

[53] Y. Habibi, L.A. Lucia, O.J. Rojas, Cellulose nanocrystals: chemistry, self-assembly, and applications.*Chemical Reviews*, **110(6)**, 3479–3500, 2010. https://doi.org/10.1021/cr100339w

[54] D. Trache, M.H. Hussin, M.K.M. Haafiz, V.K. Thakur, Recent progress in cellulose nanocrystals: sources and production. *Nanoscale*, **12(18)**, 10071-10086, 2020. https://doi.org/10.1039/D0NR04042J